Selective Guest Binding by Tailored Channels in a 3-D Porous Zinc(II)−Benzenetricarboxylate Network

O. M. Yaghi,* Charles E. Davis, Guangming Li, and Hailian Li

Contribution from the Department of Chemistry and Biochemistry, Goldwater Center for Science and Engineering, Arizona State University, Tempe, Arizona 85287-1604

Received November 13, 1996[⊗]

Abstract: Diffusion of triethylamine into an ethanol solution containing 1,3,5-benzenetricarboxylic acid (H_3BTC) and zinc(II) nitrate hexahydrate yields crystalline $Zn_2(BTC)(NO_3)\cdot(H_2O)(C_2H_5OH)_5$, which was formulated by elemental microanalysis, solid-state NMR, and single-crystal X-ray diffraction [cubic, $P2_13$, $a = 14.728(2)$ Å, $V = 3195(2)$ Å^3, $Z = 4$]. This compound possesses a 3-D structure with nearly 44% of the framework represented by an extended channel system having a 14 Å cross-section, where highly mobile ethanol and water guest molecules reside. The multidentate functionality of BTC imparts rigidity to the structure, consequently allowing the guests to be removed or exchanged without destruction of the porous framework. X-ray powder diffraction, solid-state NMR (^{13}C CP MAS and static), gas chromatography, and thermogravimetry analyses reveal that this material is highly selective to alcohols because of the coordination environment adopted by Zn(II) within its framework. Other molecular inclusions such as tetrahydrofuran, methyl ethyl ketone, acetonitrile, and acetone are not permitted into the channels, due to the specific electronic demands of the Zn(II) center and its ability to direct the inclusion process even in cases where incoming molecules have the appropriate shape and size for inclusion.

Introduction

The assembly of porous materials from organic molecule and metal-ion building blocks is an emerging area which is yielding new generations of open supramolecular architectures.[1] The pores within these materials possess sizes and shapes of a variety yet unobserved in other crystalline porous solids such as zeolites and molecular sieves. Currently, at least two challenges dealing with access to the pores of these materials remain largely unaddressed. First, the presence of interpenetrated networks has inhibited, in many cases, the preparation of large pores within the assembled structure. Second, the integrity of the synthesized framework is not maintained in the absence of guest inclusions, thus preventing study of many potentially important and interesting properties. Given the sophistication and diversity of ligand reactions and metal coordination chemistry, we believe that extensive and unparalleled opportunities exist not only for tailoring unusual porous architectures but also for addressing these issues in order to allow the incorporation of novel properties within these hybrid organic/inorganic open frameworks. For example, the presence of coordinative unsaturation around metal centers in extended crystalline solids is extremely rare, despite the fact that they have been implicated as important intermediates in a number of industrial processes involving separation of oxygen from air, and selective partial oxidation of *n*-butane and *p*-xylene.[2,3]

Here, we describe the construction of a 3-D porous and noninterpenetrated network from a highly symmetric organic unit, 1,3,5-benzenetricarboxylate (BTC), and zinc(II) ion to form crystalline $Zn_2(BTC)(NO_3)\cdot(H_2O)(C_2H_5OH)_5$. The size, conformation, and triple-bidentate functionality of BTC enhance the rigidity of the Zn−BTC framework, thus allowing access to the metal centers through a 14 Å cross-section channel system that occupies a volume constituting nearly 44% of the structure. The coordination unsaturation around the metal centers within this framework provides a unique environment for promoting the selective binding of alcohols without destruction of its porous structure. The synthetic method, structural features, and inclusion properties of this material, including the solution and solid-state behavior of the guest molecules, are presented.

Synthetic Strategy

For the construction of the targeted porous three-dimensional network, it was recognized that complete deprotonation of 1,3,5-benzenetricarboxylic acid (H_3BTC), **a**, would be essential in order to bind metal ions in a multidentate fashion as shown in **b**−**d**. This is a desirable attribute because it is expected to lead to a 3-D network, and enhance the thermal stability and rigidity of the resulting framework. We learned in earlier studies that the dimensionality of the resulting M−BTC framework is mainly dependent on the solvent used in the synthesis, and the strength of base employed for the deprotonation of H_3BTC, as summarized in Figure 1. The hydrothermal synthesis of porous 1-D frameworks utilizes acetate as a strong conjugate base for deprotonation, and water as both a solvent and a strong coordinating ligand (Figure 1a).[4] However, using a poor coordinating solvent such as ethanol, and a weak base such as pyridine for deprotonation, gives a porous 2-D structure. This is possibly due to the tendency of pyridine ($pK_a = 5.21$) to partly deprotonate H_3BTC and, in the absence of water, to strongly bind to metal ions, thereby blocking extension of the framework

[⊗] Abstract published in *Advance ACS Abstracts,* March 1, 1997.

(1) (a) Venkataraman, D.; Lee, S.; Moore, J. S.; Zhang, P.; Hirsch, K. A.; Gardner, G. B.; Covey, A. C.; Prentice, C. L. *Chem. Mater.* **1996**, *8*, 2030−2040. (b) Yaghi, O. M. In *Access in Nanoporous Materials*; Pinnavaia, T. J., Thorpe, M. F., Eds.; Plenum: New York, 1995; p 111. (c) Stein, A.; Keller, S. W.; Mallouk, T. E. *Science* **1993**, *259*, 1558−1564. (d) Fagan, P. J.; Ward, M. D. *Sci. Am.* **1992**, *267*, 48−54. (e) Bein, T. *Supramolecular Architecture: Synthetic Control in Thin Films and Solids;* American Chemical Society: Washington, DC, 1992. (f) Iwamoto, T. In *Inclusion Compounds*; Atwood, J. L., Davies, J. E. D., MacNicol, D. D., Eds.; Oxford: New York, 1991; Vol. 5, pp 177−212. (g) Hoskins, B. F.; Robson, R. *J. Am. Chem. Soc.* **1990**, *112*, 1546−1554. (h) Lu, J.; Harrison, W. T. A.; Jacobson, A. J. *Angew. Chem., Int. Ed. Engl.* **1995**, *34*, 2557−2559.

(2) Ramprasad, D.; Pez, G. P.; Toby, B. H.; Markley, T. J.; Pearlstein, R. M. *J. Am. Chem. Soc.* **1995**, *117*, 10694−10701.

(3) Centi, G.; Triffiro, F.; Ebner, J. R.; Franchetti, V. M. *Chem. Rev.* **1988**, *88*, 55−80.

(4) Yaghi, O. M.; Li, H.; Groy, T. L. *J. Am. Chem. Soc.* **1996**, *118*, 9096−9101.

S0002-7863(96)03947-9 CCC: $14.00

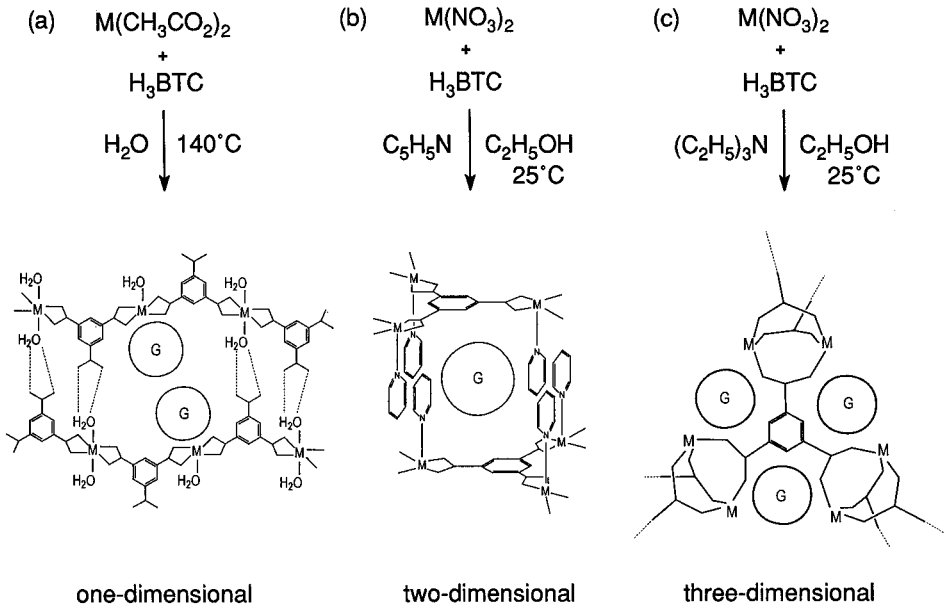

Figure 1. A schematic representation of (a) 1-D (b) 2-D, and (c) 3-D structures produced by reacting metal ions (M) with 1,3,5-benzenetricarboxylic acid (H_3BTC), and the dependence of their dimensionality on the solvent and base employed in the reaction. For clarity, all hydrogen atoms have been omitted from the structures, with the corners representing carbon and oxygen atoms of BTC.

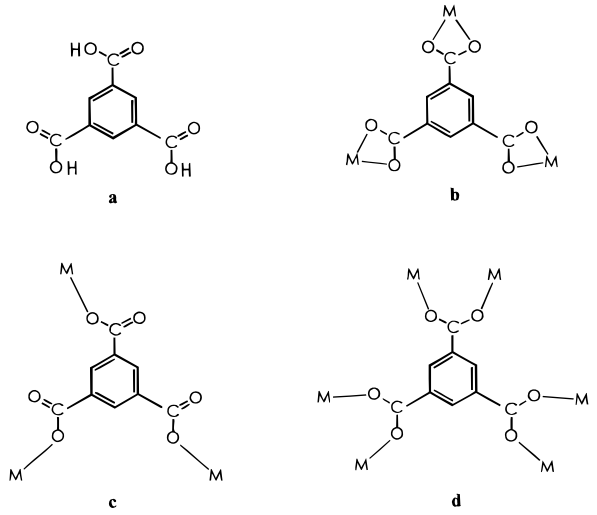

into the third dimension (Figure 1b).[5] It was postulated that a 3-D network would be achieved under similar conditions upon employing a stronger base such as triethylamine ($pK_a = 11.01$) with sufficient strength to completely deprotonate H_3BTC, but with poor affinity for binding to metal ions. The success of this approach results in a porous 3-D extended network having a rigid architecture which is held together by the multidentate functionalities of BTC as shown in Figure 1c.

Experimental Section

Materials and Methods. Zinc(II) nitrate hexahydrate and 1,3,5-benzenetricarboxylic acid were purchased from Aldrich Chemical Co. and used as received, without further purification. Elemental microanalysis of all products was performed on crystalline samples by the School of Chemical Sciences Microanalytical Laboratory at the University of Illinois-Urbana, and by the Arizona State University Materials Facility using a Perkin-Elmer 2400 CHNS analyzer. Thermogravimetric (TG) analysis was performed under He at a scan rate of 0.5 °C/min using a Setaram TG92 system.

Fourier transform infrared (FT-IR) spectra were measured from KBr pellets using a Nicolet FT-IR Impact 400 system. Absorptions are described as follows: very strong (vs), strong (s), medium (m), weak (w), shoulder (sh), and broad (br). Solid-state ^{13}C NMR spectra were recorded on a Varian Unity Plus-400 spectrometer using a cross-polarization magic angle spinning (CP MAS) probe with a 5 mm silicon nitride rotor at spin rates ranging from 0 to 11 000 Hz. Chemical shifts were referenced externally to tetramethylsilane (δ 0 ppm) using solid hexamethylbenzene (δ 17.3 ppm) as a secondary reference. X-ray powder diffraction (XRPD) data were recorded on a Rigaku D/Max-IIB diffractometer at 50 kV, 30 mA for Cu Kα ($\lambda = 1.5406$ Å), with a scan speed of 2 deg/min and a step size of 0.02° in 2θ. XRPD data are reported for the most prominent lines with *d*-spacings in angstroms and the relative intensities placed in parentheses followed by their *hkl* assignments. The calculated XRPD patterns were produced using the SHELXTL-XPOW program and the single-crystal data.

Gas chromatographic (GC) experiments were conducted using a Varian 3700 gas chromatograph having 1/8 in. × 6 ft packed columns at temperatures ranging from 80 to 230 °C under a He flow rate of 20 cm^3/min. An Alltech Carbograph 1NKA column was used for the analysis involving 1-pentanol, 1-heptanol, and 4-*tert*-butyl phenol guest inclusions. For all other inclusions an Alltech Porapak R column was employed. A flame ionization detector was used in conjunction with a strip chart recorder. Peak integrations were performed manually for each sample.

Preparation of Compounds. The synthetic methods used to obtain microcrystalline and large single-crystal samples of the compounds, including their initial characterization, are described here. Unless otherwise indicated all reactions and purification steps were performed under aerobic conditions.

$Zn_2(BTC)(NO_3)\cdot(H_2O)(C_2H_5OH)_5$. An absolute ethanol mixture (10 mL) of zinc(II) nitrate hexahydrate (0.30 g, 1.00 mmol) and the acid form of BTC (H_3BTC) (0.105 g, 0.500 mmol) was added into a small vial, which was placed in a larger vial containing triethylamine (2 mL). The larger vial was sealed and left undisturbed at room temperature for 6 d. The resulting white solid near the solution/air interface was decanted, and the colorless large cube-shaped crystals at the bottom of the vial were isolated and then washed with 3 × 10 mL of absolute ethanol to give 0.045 g (14%) of product. Although this compound is insoluble in water and common organic solvents such as ethanol, acetonitrile, chloroform, tetrahydrofuran, acetone, and *N*,*N*-dimethylformamide, it loses solvent upon exposure to the atmosphere. Anal. Calcd for $C_{19}H_{35}NO_{15}Zn_2 = Zn_2(BTC)(NO_3)\cdot(H_2O)(C_2H_5OH)_5$: C, 35.20; H, 5.44; N, 2.16; Zn, 20.17. Found: C, 35.30; H, 5.54; N, 2.06; Zn, 19.77. FT-IR (KBr, 3500−400 cm^{-1}): 3400 (br), 3194 (sh), 2658 (br), 2428 (w), 2402 (w), 2347 (w), 1763 (w), 1619 (s), 1552 (s), 1435 (s), 1385 (vs), 1373 (sh), 1359 (sh), 1209 (w), 1112 (w), 933 (w), 911 (w), 829 (w), 758 (m), 739 (m), 723 (sh), 619 (w),

(5) Yaghi, O. M.; Li, G.; Li, H. *Nature* **1995**, *378*, 703−706.

Table 1. XRPD Data for $Zn_2(BTC)(NO_3)\cdot(H_2O)(C_2H_5OH)_5$ Starting Material, **1**, Regenerated after Partial Evacuation by Exposure to Ethanol, **2**, and $Zn_2(BTC)(NO_3)\cdot(H_2O)_{0.5}(C_2H_5OH)_{0.5}(DMF)_{2.5}$, **3**, Including *hkl*, *d*-Spacing (Å), Intensity (I/I_o), and Full Width at Half-Maximum (FWHM)

	1					**2**			**3**		
	calcd		obsd								
hkl	*d*-spacing	I/I_o (%)	*d*-spacing	I/I_o (%)	FWHM	*d*-spacing	I/I_o (%)	FWHM	*d*-spacing	I/I_o (%)	FWHM
011	10.414	99	10.394	60	0.172	10.419	29	0.336	10.018	70	0.194
111	8.503	100	8.483	100	0.192	8.499	100	0.397	8.185	100	0.212
102	6.586	9	6.573	1	0.318	6.563	10	0.339	6.339	4	0.295
112	6.013	25	6.013	5	0.257	6.021	18	0.898	5.779	5	0.257
022	5.207	11	5.200	7	0.236	5.193	15	0.318	5.013	22	0.213
103	4.657	15	4.638	10	0.238	4.648	16	0.737	4.485	5	0.316
113	4.441	11	4.432	2	0.298	4.432	10	0.477	4.275	3	0.296
223	3.572	17	3.562	8	0.197	3.562	22	0.358	3.440	3	0.258
214	3.241	6	3.202	2	0.277	3.207	8	0.536	3.093	1	0.355

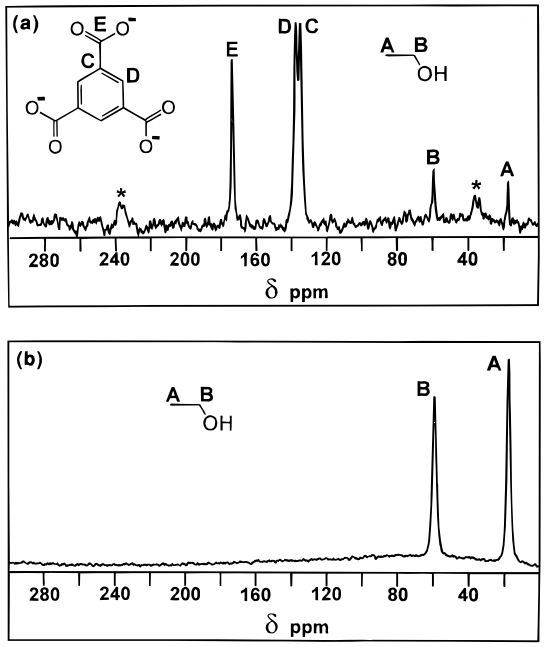

Figure 2. Solid-state NMR spectra of $Zn_2(BTC)(NO_3)\cdot(H_2O)(C_2H_5OH)_5$ (a) as ^{13}CP MAS and (b) under static nonspinning conditions. The peaks marked with an asterisk indicate sidebands.

560 (w), 463 (w), 434 (w). ^{13}C CP MAS NMR: δ 134.1 and 136.6 (s, ***C***$_6$H$_3$(COO)$_3$), 172.7 (s, C$_6$H$_3$(***C***OO)$_3$), 59.0 (s, CH$_3$***C***H$_2$OH), and 17.4 (s, ***C***H$_3$CH$_2$OH). ^{13}C solid-state static NMR: δ 59.0 (s, CH$_3$***C***H$_2$OH) and 17.5 (s, ***C***H$_3$CH$_2$OH). Typical NMR spectra are shown in Figure 2.

The phase purity of the bulk product was confirmed by comparison of the observed and calculated XRPD patterns. Calculated and observed XRPD patterns including *d*-spacing, I/I_0, *hkl*, and line widths for the most prominent are shown in Table 1.

Thermogravimetric analysis performed under a flow of helium gas on a 24.39 mg sample showed a weight loss of 7.28 mg (29.9%) after 75 h at 25 °C, which is equivalent to the loss of 4 ethanol and 0.5 water molecules per formula unit (calcd 29.8%). A total weight loss of 9.88 mg (40.5%) is achieved at 215 °C, which is equivalent to the loss of five ethanol and one water molecules per formula unit (calcd 38.3%). Further heating of the sample results in the formation of ZnO at 460 °C, as indicated by the total weight loss of 19.1 mg (75.1%) (calcd 74.9%) and the XRPD pattern of the resulting solid.

$Zn_2(BTC)(NO_3)\cdot(H_2O)_{0.5}(C_2H_5OH)$. Crystalline samples of freshly isolated and pure $Zn_2(BTC)(NO_3)\cdot(H_2O)(C_2H_5OH)_5$ were subjected to a dinitrogen stream at room temperature for 1 d to yield the desired product, as indicated by the observed weight loss in the TGA experiment (*vide supra*). Anal. Calcd for $C_{11}H_{10}NO_{10.5}Zn_2$: C, 29.04; H, 2.22; N, 3.08. Found: C, 29.34; H, 2.65; N, 2.96. Observed XRPD: broadened and less intense lines relative to the starting material. The most intense *hkl* lines (011, 111, 112, 022, 103) can still be discerned; however, due to the extent of line broadening, no accurate line widths can be obtained. These lines sharpen and a full XRPD pattern similar to that of the unevacuated material is established as this material is exposed to ethanol vapor. The data for this regenerated material are shown in Table 1.

$Zn_2(BTC)(NO_3)\cdot(H_2O)_{0.5}(C_2H_5OH)_{0.5}(DMF)_{2.5}$. Large transparent colorless crystals of nearly 0.2 × 0.2 × 0.2 mm size of the unevacuated parent solid were immersed in *N*,*N*-dimethylformamide (DMF) for 5−15 min at room temperature and then filtered. Anal. Calcd for $C_{17.5}H_{24.5}N_{3.5}O_{12.5}Zn_2$: C, 34.20; H, 4.02; N, 7.98. Found: C, 34.06; H, 4.01; N, 8.20. ^{13}C CP MAS NMR: δ 134.2 and 136.6 (s, ***C***$_6$H$_3$(COO)$_3$), 173.3 (s, C$_6$H$_3$(***C***OO)$_3$), 58.6 (s, CH$_3$***C***H$_2$OH), 17.7 (s, ***C***H$_3$CH$_2$OH), 165.8 (s, (CH$_3$)$_2$N***C***(O)H), and 36.9 and 31.8 (s, (***C***H$_3$)$_2$NC(O)H). ^{13}C solid-state static NMR: δ 165.8 (s, (CH$_3$)$_2$N***C***(O)H), and 36.9 and 31.8 (s, (***C***H$_3$)$_2$NC(O)H).

Examination of the resulting crystalline material under an optical microscope showed that the crystal morphology is maintained with some loss of transparency. However, it remains crystalline according to its XRPD pattern and its close agreement with that of the parent solid (compare parts a and b of Figure 3). Observed XRPD parameters are shown in Table 1. Calculated cell parameters from observed XRPD: assuming a cubic cell, a = 14.266 Å.

Calculated Pore Volume. To approximate the pore volume, it was necessary to calculate an estimate for the average volume of the non-hydrogen atoms. This was accomplished by subtracting the volume of the hydrogen atoms from the total cell volume, and then the remaining volume was divided by the number of non-hydrogen atoms in the cell.[6] The result was multiplied by the number of non-hydrogen atoms in the pores, to which the volume of the hydrogen atoms in the pores was added to give the total volume of molecules occupying the pores. This value was used as the calculated pore volume. Of course, similar analysis can be applied for calculating the volume occupied by the framework and then subtracting that from the total cell volume to give the pore volume. In the absence of two ethanol and one water molecules per formula unit, the calculated pore volume is 19.1%. Complete removal of five ethanol and one water molecule per formula unit gave a calculated pore volume of 43.6%.

NMR Guest Binding Survey. Samples of the as-synthesized or the evacuated solid were immersed at room temperature for 5−15 min in solutions containing potential guest molecules. The solid was filtered and washed very quickly with ethanol (3 × 10 mL) under suction through a coarse fritted funnel, prior to acquiring its ^{13}C CP MAS and static solid-state NMR spectra. Typically, spectra of the spinning samples showed resonances due to BTC and the guest species; however, only resonances due to the guests were observed for the static samples (Figure 2). Inclusion of methanol, ethanol, 1-propanol, isopropyl alcohol, 1-butanol, *tert*-butyl alcohol, and *N*,*N*-dimethylformamide was observed at the expected chemical shifts for unbound solvents. No NMR evidence was found for the inclusion of 4-*tert*-butyl phenol, chloroform, 1,2-dichloroethane, acetonitrile, nitrobenzene, cyanobenzene, toluene, methyl ethyl ketone, or acetone.

(5) The covalent radius for hydrogen was used: *Inorganic Chemistry: Principles of Structure and Reactivity, 4th ed.*; Huheey, J. E., Keiter, E. A., Keiter, R. L., Eds.; HarperCollins: New York, 1993; p 292.

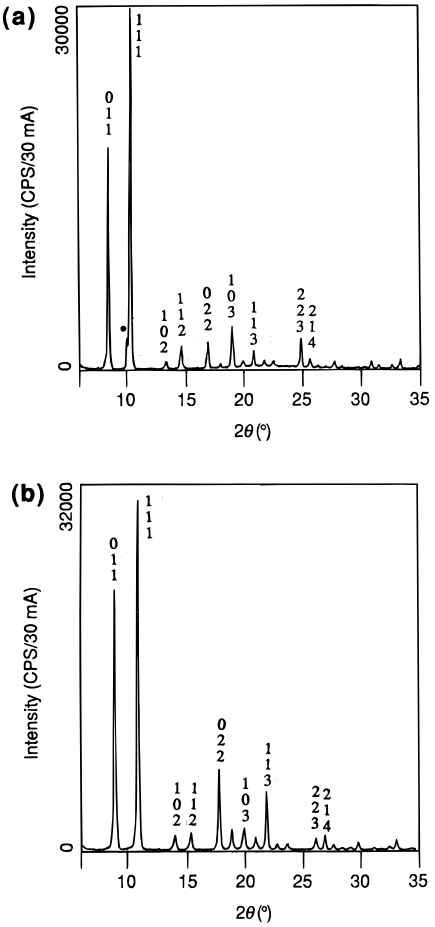

Figure 3. Comparison of the X-ray powder diffraction patterns of the (a) unevacuated material, $Zn_2(BTC)(NO_3)\cdot(H_2O)(C_2H_5OH)_5$, and (b) its inclusion product, $Zn_2(BTC)(NO_3)\cdot(H_2O)_{0.5}(C_2H_5OH)_{0.5}(DMF)_{2.5}$. The dot in (a) represents a slight lowering of symmetry due to the rapid loss of ethanol from the solid.

GC Competition Binding Studies. In a typical experiment, solutions of known concentrations were prepared by mixing equimolar amounts of potentially competing guest molecules in approximately 1% solutions (w/w) in toluene (1.00 mL). To this mixture was added a stoichiometric amount of the host material (0.100 or 0.050 g) in the as-synthesized form to yield a heterogeneous mixture. Immediate GC analysis of the supernatant revealed changes in the concentrations of certain mixture components relative to those observed prior to the addition of the host solid. The results for a number of guest mixtures are summarized in Table 2. To confirm the initial and to calculate the final concentrations for each guest solvent, standard plots of area versus concentration were prepared by measuring the areas corresponding to successive dilutions (3.0−0.2% w/w) of that guest solvent. These produced linear plots for each potential guest having correlation coefficients greater than 0.94. The initial concentrations interpolated from such plots were consistent within a ±0.01 M range of those originally calculated during solution preparation. The final concentrations were also interpolated from these plots for each potential guest.

Absorption−Desorption Cycles. The reversible binding of DMF was confirmed by immersing a solid sample of $Zn_2(BTC)(NO_3)\cdot(H_2O)_{0.5}(C_2H_5OH)_{0.5}(DMF)_{2.5}$ into a 1% solution (w/w) of methanol/ethanol/DMF in toluene, which resulted in a decreased amount of alcohols accompanied by an increase in that of DMF as observed by the GC trace of the supernatant. In another experiment, the parent unevacuated solid was immersed in a solution containing 1% 1-propanol in toluene. An immediate GC analysis of the supernatant revealed an increase in the amount of ethanol accompanied by a decrease in that of 1-propanol. An identical trend was found when the resulting solid was subjected to a solution containing 1% methanol in toluene.

X-ray Data Collection and Reduction. An X-ray single-crystal analysis study was undertaken on $Zn_2(BTC)(NO_3)\cdot(H_2O)(C_2H_5OH)_5$.

Table 2. Competitive Binding of Molecular Guests into the Host $Zn_2(BTC)(NO_3)\cdot(H_2O)(C_2H_5OH)_5$

			amt of guest (mmol × 10^3) in supernatant	
no.	potential guest	amt. of host (mmol × 10^3)	before addition of host	after addition of host
I	CH_3OH	154	158	61
	n-C_3H_7OH		163	103
	n-C_4H_9OH		158	95
II	C_2H_5OH	154	0	281
	n-C_4H_9OH		118	80
	t-C_4H_9OH		114	64
III	CH_3CN	78	166	171
	C_2H_5OH		0	153
	C_4H_8O (THF)		166	149
	C_6H_6		171	171
IV	C_2H_5OH	78	0	153
	$CH_3CH_2C(O)CH_3$		118	119
	n-C_4H_9OH		117	32
V	C_2H_5OH	78	0	153
	t-$C_5H_{11}OH$		96	51
	n-$C_7H_{15}OH$		96	64

Table 3. Crystallographic Data for $Zn_2(BTC)(NO_3)\cdot(H_2O)(C_2H_5OH)_5$

formula	$C_{19}H_{35}NO_{15}Zn_2$	*Z*	4
M	648.22	*V* (Å^3)	3195(2)
crystal system	cubic	d_{calcd} (g/cm^3)	1.348
space group	$P2_13$	μ, mm^{-1}	1.56
a (Å)	14.728(4)	*R* (R_w)	0.064 (0.067)

The experimental details for the structure determination are given in Table 3. A nearly cube-shaped colorless single crystal (0.28 mm on an edge) was separated from the reaction product and quickly sealed inside a thin-walled glass capillary. Data were collected on a computer-controlled four-circle Nicolet (Siemens) autodiffractometer using graphite-monochromated Mo Kα radiation and full 1.20° wide ω scans to a maximum of $2\theta = 43.0°$, giving 707 independent absorption-corrected reflections. Lattice parameters were obtained from least-squares analyses of 15 computer-centered reflections with $2\theta > 15°$. The raw intensity data were converted to structure factor amplitudes and their estimated standard deviations by correction for scan speed, background, and Lorentz and polarization effects using the XDISK facility within the SHELXTL PC package. The data were corrected for absorption using ψ-scan data from three reflections covering the range of data collection with resultant maximum and minimum transmission values of 1.000 and 0.953. The compound crystallized in the cubic system, and statistics identified the space group as $P2_13$ (No. 198) which was consistent with all stages of the subsequent structure determination and refinement.

Structure Solution and Refinement. The structure was solved using Direct Methods techniques with the Siemens SHELXTL-PC software package as modified at Crystalytics Co. The resulting structural parameters have been refined to convergence {R_1(unweighted, based on F) = 0.064 for 348 independent absorption-corrected reflections having 2Θ(Mo Kα) < 43.0° and $I > 2.5\sigma(I)$} using counter-weighted full-matrix least-squares techniques and a structural model which incorporated anisotropic thermal parameters for the metal atoms and oxygen atoms O1, O2, and O3 and isotropic thermal parameters for the remaining non-hydrogen and included hydrogen atoms.

The methyl group of the coordinated ethanol (C5 and its hydrogens) was refined as a rigid rotor with sp^3-hybridized geometry and a C−H bond length 0.96 Å. The refined positions for the rigid rotor methyl group gave C−C−H angles which ranged from 104° to 114°. Additional ligand hydrogen atoms bonded to carbon were included in the structure factor calculations as idealized atoms (assuming sp^2- or sp^3-hybridization of the carbon atoms and a C−H bond length of 0.96 Å) riding on their respective carbon atoms. The hydroxyl proton on the coordinated ethanol molecule could not be located from difference Fourier syntheses and was not included in the structural model. The

isotropic thermal parameter of each included hydrogen atom was fixed at 1.2 times the equivalent isotropic thermal parameter of the carbon atoms to which it is covalently bonded. Hydrogen atoms on the water and ethanol solvent molecules present in the lattice were also not included in the structural model.

The nitrate anion appears to be approximately bidentate and statistically disordered about the crystallographic 3-fold axis of the unit cell. This 3-fold axis passes through both zinc atoms and the noncoordinated oxygen atom (O5) of the disordered nitrate anion. Oxygen atom O4 and the nitrogen atom N1 lie off this 3-fold axis and were included in the refinement with occupancy factors of 0.67 and 0.33, respectively. Since N1 was within 0.49 Å of its C_3-related symmetry equivalents, its positional parameters could not be satisfactorily refined in least-squares cycles. These positional parameters were therefore fixed at the Fourier values.

The elemental analysis as well as difference Fourier electron density maxima (calculated for a structural model which only included zinc atoms and non-hydrogen atoms of ligands coordinated to them) indicated that the water and ethanol solvent molecules of crystallization were statistically disordered about a point on the crystallographic C_3-axis at approximately 1/3, 1/3, 1/3 in the unit cell. The following three criteria were taken as being consistent with one-third of the sites around the C_3-axis being occupied by water molecules and two-thirds being occupied by ethanol solvent molecules of crystallization: (1) difference Fourier peak heights, (2) least-squares refined occupancy factors for the non-hydrogen atoms of these solvent molecules, and (3) metrical parameters for possible intramolecular (those for ethanol) and intermolecular hydrogen bonds. Both of these solvent molecules have their oxygen atoms favorably oriented for forming hydrogen bonds with neighboring oxygen atoms of coordinated ethanol and/or nitrate ligands. Occupancy factors of 0.33 and 0.67 were therefore used for the non-hydrogen atoms of the water and ethanol molecules of crystallization, respectively. Carbon−oxygen and carbon−carbon bond lengths and the O···C(methyl) separations within the coordinated and solvent ethanol molecules were restrained to have values which were (0.93, 1.00, and 1.63, respectively) multiples of a least-squares refineable free variable for each molecule. This free variable refined to a value of 1.68(4) and 1.41(7) for the coordinated and solvent ethanols, respectively.

Results and Discussion

Synthesis and Structure of $Zn_2(BTC)(NO_3)\cdot(H_2O)(C_2H_5OH)_5$. Large cube-shaped crystals of this compound are produced at room temperature upon diffusing triethylamine into a clear ethanol solution containing $Zn(NO_3)_2\cdot 6H_2O$ and H_3BTC in a 2:1 mole ratio. Bulk samples and single crystals of this material lose solvent upon exposure to air and nonalcoholic gaseous or liquid media. Elemental microanalysis performed on freshly prepared samples gave the indicated formulation for the compound. Its FT-IR spectrum showed the expected absorptions for the symmetric and asymmetric vibrations of BTC (1552 and 1435 cm^{-1}), a hydrogen-bonded water and ethanol (3400, 3194, and 1619 cm^{-1}), and nitrate (1385−1359 cm^{-1}).[7,8] It showed no absorptions for any protonated BTC (1730−1690 cm^{-1}), indicating the complete deprotonation of H_3BTC by the addition of triethylamine to the reaction mixture.

A single-crystal X-ray diffraction study revealed an extended 3-D porous framework formulated as $Zn_2C_6H_3(COO)_3(NO_3)\cdot(H_2O)(C_2H_5OH)_5$, which is consistent with that derived from elemental microanalysis. Crystal data and selected bond lengths and angles are given in Tables 3 and 4, respectively. The fundamental building unit of the crystal structure is shown in Figure 4. It is composed of two different zinc(II) centers (Zn1, Zn2) that are bridged by three carboxylates (O1, O2; O1A, O2A; O1B, O2B) of three separate BTC units, where all the symmetry equivalent O1 atoms are linked to Zn1, and all the symmetry equivalent O2 atoms are linked to Zn2. Progression of the structure in the crystal employs this unit and its linkage motif using the remaining carboxylate oxygens (O1C, O2C; O1E, O2E; O1H, O2H; and O1D, O2D; O1F, O2F; O1G, O2G) on each BTC unit. In this way, each BTC unit acts as a hexamonodentate unit, linking three pairs of zinc atoms to yield a tightly held framework, where each zinc atom has attained a trigonal pyramidal geometry with respect to its coordination to the BTC. The remaining positions on Zn1 and Zn2 are, respectively, occupied by three ethanol ligands (O3, O3A, O3B) and one bidentate nitrate (O4, O4A) ligand. The remaining ethanol (O1S, C1S, C2S) and water (O1W) molecules are isolated from and are not bound to the Zn−BTC building unit. It is instructive to view this unit as a trigonal bipyramidal polyhedron, where the axial positions are occupied by zinc atoms, with one being capped by three ethanol ligands and the other by a nitrate ligand. The equatorial positions and the edges of the polyhedron can be, respectively, viewed as representing the carbon (C1, C1A, C1B) and oxygen (O1, O1A, O1B and

Table 4. Selected Bond Lengths and Angles for $Zn_2(BTC)(NO_3)\cdot(H_2O)(C_2H_5OH)_5$

Distances (Å)			
Zn(1)−O(1)	2.03(2)	Zn(2)−O(2)	1.96(2)
Zn(1)−O(3)	2.14(2)	Zn(2)−O(4)	2.14(6)
O(1)−C(1)	1.20(4)	O(2)−C(1)	1.28(3)
N(1)−O(4)	1.02(6)	N(1)−O(5)	1.29(6)
Angles (deg)			
O(3)Zn(1)O(1B)	87.3(9)	O(4)Zn(2)O(4B)	41.9(27)
O(3)Zn(1)O(3B)	87.3(10)	O(4)Zn(2)O(2B)	89.6(18)
O(1)Zn(1)O(3)	88.9(8)	O(4)Zn(2)O(2A)	90.4(19)
O(1)Zn(1)O(1B)	96.1(7)	O(2)Zn(2)O(2B)	115.3(4)
O(3)Zn(1)O(1A)	173.6(9)	O(2)Zn(2)O(4)	127.1(17)
Zn(1)O(1)C(1)	139(2)	Zn(2)O(2)C(1)	118(2)
O(1)C(1)O(2)	130(2)	Zn(1)O(3)C(4)	135(2)
O(1)C(1)C(2)	118(2)	O(3)C(4)C(5)	116(4)
O(2)C(1)C(2)	112(2)	Zn(2)O(4)N(1)	106(4)
		Zn(2)O(4A)N(1)	95(3)

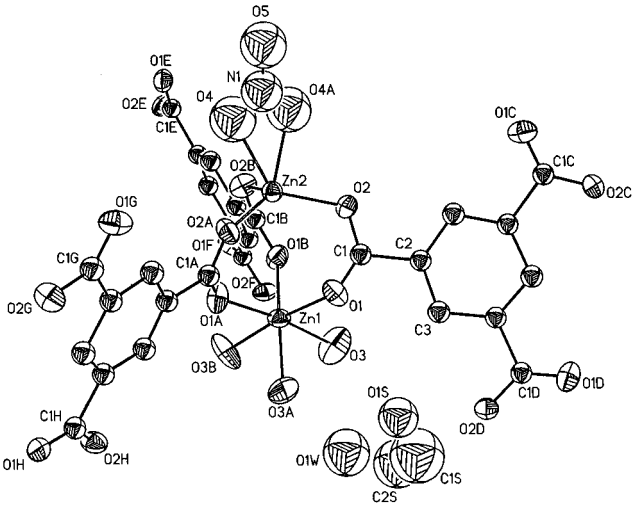

Figure 4. A perspective drawing of the building block unit for the structure of $Zn_2(BTC)(NO_3)\cdot(H_2O)(C_2H_5OH)_5$, with all the non-hydrogen atoms represented by 30% thermal ellipsoids. The coordinated nitrate anion is statistically disordered about the crystallographic 3-fold axis of the unit cell which passes through Zn1, Zn2, and O5; only one orientation for the nitrate anion is shown. All the hydrogen atoms have been omitted, and only the oxygen atoms (O3, O3A, and O3B) of the ethanol ligands are shown. Atoms with additional A−H labels are symmetry related to atoms labeled without such subscripts.

(6) (a) Brzyska, W.; Sadowski, P. *Pol. J. Chem.* **1987**, *61*, 273−279. (b) Brzyska, W.; Wolodkiewicz, W. *Pol. J. Chem.* **1986**, *60*, 697−702. (c) Wieghardt, K. *JCS Dalton* **1973**, 2548−2552. (d) Bellamy, L. J. *The Infrared Spectra of Complex Molecules*; **1958**, Wiley (New York).

(7) Gordon, A. J.; Ford, R. A. *The Chemist's Companion: A Handbook of Practical Data, Techniques, and References*, **1972**, Wiley (New York).

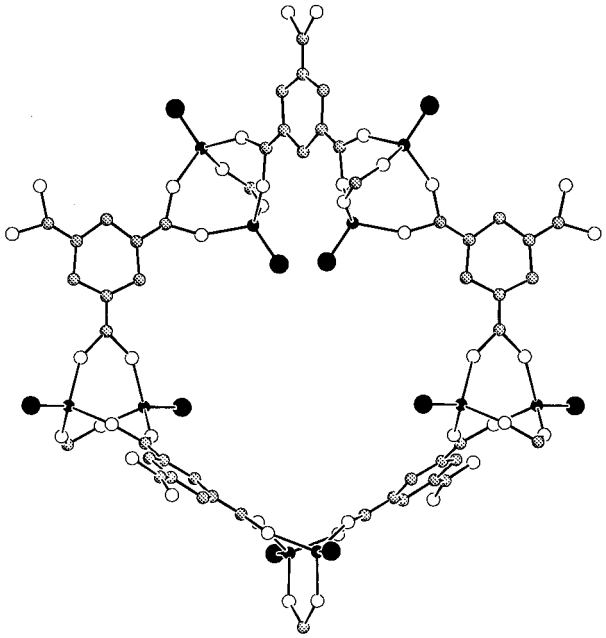

Figure 5. Secondary building block in the porous Zn−BTC framework of $Zn_2(BTC)(NO_3)\cdot(H_2O)(C_2H_5OH)_5$, where the trigonal bipyramidal polyhedron and BTC are linked together to form a large 10-membered ring structure. The nitrate and ethanol ligands alternating around the ring are represented by large dark spheres to emphasize the manner in which they point to the center of the void. Other spheres represent the framework atoms as follows: Zn (dark small); O (open) and C (shaded). All hydrogen atoms have been omitted for clarity.

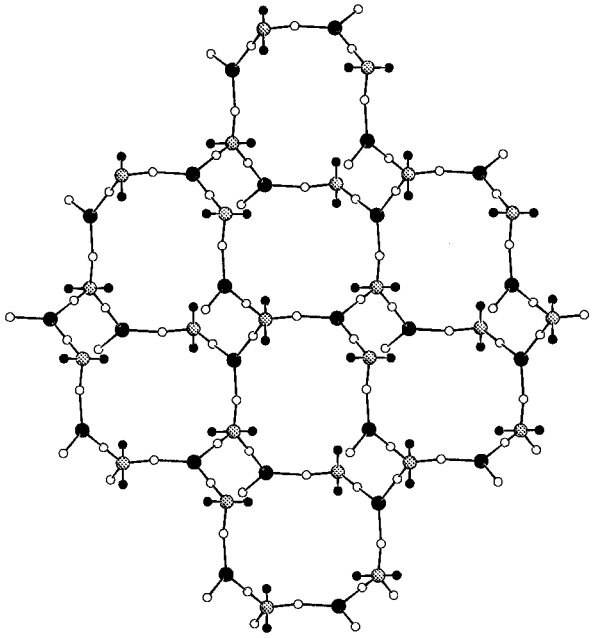

Figure 6. A view of the topology of ring (Figure 5) linkage in the Zn−BTC framework, where the center of the trigonal bipyramids and BTC are represented by large dark and shaded spheres, respectively. The zinc and carboxyl carbon atoms are shown as dark and open small spheres, respectively.

O2, O2A, O2B) atoms of the bridging carboxylates. This arrangement leads to a large 10-membered ring composed of five such trigonal bipyramids linked together by five BTC units as shown in Figure 5, where the ethanol and nitrate ligand positions point away from the ring into the center of the voids—an aspect of the structure that leads to unique guest binding behavior (*vide infra*). The overall crystal structure of this material results from fusing such rings together as shown for a fragment of the structure in Figure 6. Extension of the structure in the third dimension gives a 3-D porous Zn−BTC network as shown using a simplified view in Figure 7. Here, the three ethanol and one nitrate ligands bound to Zn1 and Zn2 point toward the center of the channels, where the remaining two ethanol and one water molecules reside as guest inclusions. The nitrate ions are bound tightly to the zinc to give a Zn2−O4 distance of 2.14(6) Å, which does not allow for their ion exchange. It should be noted that the low precision of the final bond distances and angles is not unexpected given the inherent disorder of the guest water and all the ethanol molecules including those bound to zinc.

Guest Removal and Selective Binding. Close examination of the channels revealed that the bound ethanol molecules form weak interactions to zinc (Zn1−O3 = 2.14(2) Å), while the unbound ethanol and water molecules form weak hydrogen bonds to the ethanol ligands (O3···O1S = 2.60(7), O3···O1W = 2.93(8) Å), carboxylate (O2D···O1S), and nitrate (O4···O1SE = 3.14(9) Å).[9] To access the channels, it would be imperative that at least unbound ethanol and water be removed since in their absence the diameter of the channels is expected to be approximately 9 Å and the free pore volume 19.1% of the structure. Removal of the bound ethanol molecules would increase those values to 14 Å and 43.6%, respectively, and would allow exploitation of the metal reaction chemistry in connection to the feasibility of binding new guest molecules.

A thermogravimetric study performed on a freshly prepared sample revealed that most bound and unbound ethanol can be removed from the channels at room temperature and atmospheric pressure prior to heating the sample. A total of 4 ethanol and 0.5 water molecules per formula unit can be removed according to the observed weight loss, and as formulated by elemental microanalysis, which gave $Zn_2(BTC)(NO_3)\cdot(H_2O)_{0.5}(C_2H_5OH)$. The XRPD pattern of this solid showed that the most prominent peaks are only broadened relative to the XRPD of the parent solid (see the Experimental Section and Table 1), which indicates that the structural integrity of its Zn−BTC framework is maintained. It is worth noting that the structure retains its original form as the solid is exposed to ethanol or other alcohols as evidenced by the sharpening of the XRPD pattern lines.

The facility with which most of the bound and unbound ethanol can be removed at room temperature coupled to their exhibited disordered behavior led us to believe that they had high mobility within the channels. This was confirmed by a ^{13}C CPMAS NMR study on the original solid, which showed three peaks at δ 172.8, 136.6, and 134.1 ppm due to BTC and two peaks at δ 59.0 and 17.4 ppm due to ethanol as shown in Figure 2. When the spectrum is acquired without spinning, the BTC peaks completely disappear and, as expected for mobile inclusions,[10] the position of the two ethanol peaks remain unaltered with minimal broadening of their linewidth. Therefore, in the following discussion, no distinction will be made between guest ethanol and bound ethanol since both TG and NMR analysis show that they are indistinguishable and most likely are involved in a dynamic exchange process.

The mobility of ethanol within the channels has significant implications on the inclusion chemistry of this framework, as it renders easy access to zinc coordination sites within the channels. Solid-state NMR experiments analogous to those described above were performed on either the starting material

(9) (a) Desiraju, G. R. *Crystal Engineering: The Design of Organic Solids*; Elsevier: New York, 1989. (b) Emsley, J. *Chem. Soc. Rev.* **1989**, *91*.

(10) Gies, H. In *Inclusion Compounds*; Atwood, J. L., Davies, J. E. D., MacNicol, D. D., Eds.; Oxford: New York), 1991; Vol. 5, pp 1−36.

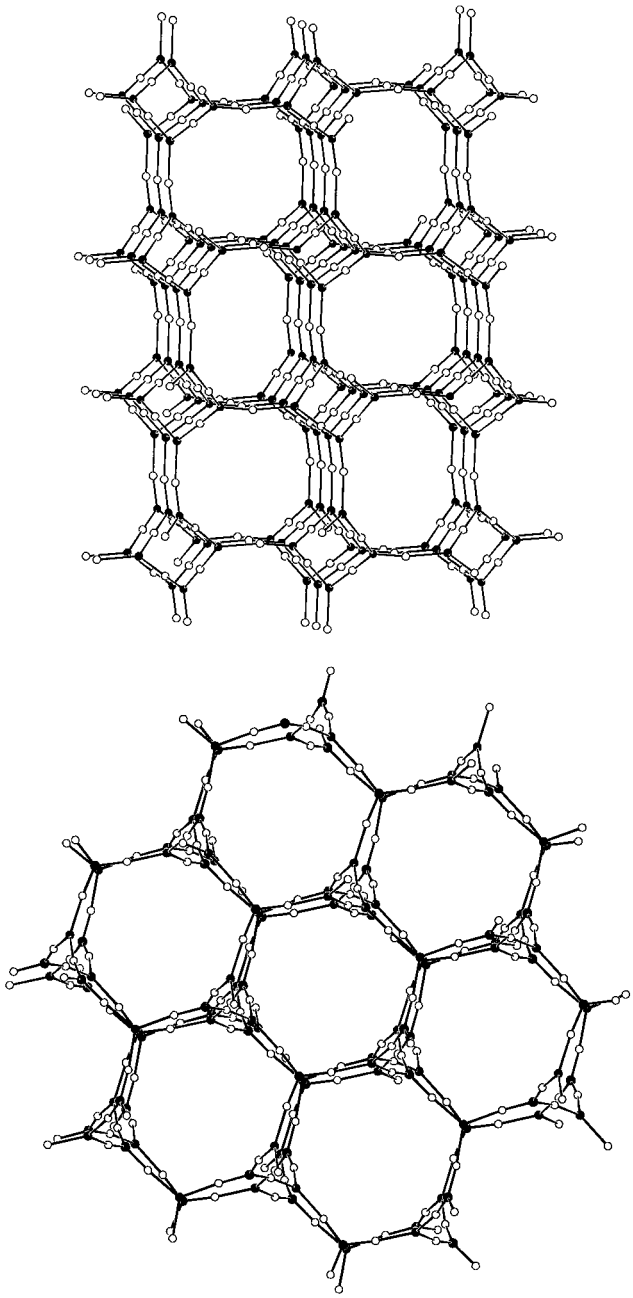

Figure 7. Topology of the 3-D, Zn−BTC porous framework in crystalline $Zn_2(BTC)(NO_3)\cdot(H_2O)(C_2H_5OH)_5$ shown along (a, top) the crystallographic *z*-axis and (b, bottom) along the 3_1 axis, where only the centers of the trigonal bipyramids and BTC are shown as dark spheres connected to the carboxylate carbon atoms (open spheres).

or the evacuated solid. They showed successful binding of small nonhindered alcohols such as methanol, ethanol, 1-propanol, isopropyl alcohol, 1-butanol, and *tert*-butyl alcohol. No NMR evidence was found for the binding of sterically hindered alcohols such as *t*-butylphenol or nonalcoholic molecules such as chloroform, 1,2-dichloroethane, acetonitrile, nitrobenzene, cyanobenzene, toluene, acetone, and methyl ethyl ketone. It appears that the affinity toward nonsterically hindered alcohols is due to the precise demands of the zinc(II) coordination sites for alcohols, as other molecules of the proper size and shape but with the different functional groups do not penetrate the channels. Additionally, the ability of alcohols to hydrogen bond to the oxygens of BTC and nitrate as determined by the single-crystal X-ray structure may play an important role in the selectivity toward the alcohol functionality. It is worth noting that DMF is the only tested nonalcoholic molecule that binds to this material with an affinity similar to that observed for alcohols. The reasons for this observation are not well-understood. Perhaps the strong affinity of DMF to hydrogen-bond to water gives it the required hydroxyl functionality for favorable inclusion; however, it remains that this framework shows a striking selectivity toward alcohols. This was confirmed by performing competition binding experiments using gas chromatography techniques, which were done by adding the as-synthesized solid to a toluene solution containing a 1% liquid mixture of potential guests to yield a heterogenous mixture.

Comparison of the initial concentrations of guests to their corresponding final concentrations is shown in Table 2. It is immediately apparent that alcohol guest molecules are highly favored over nonalcoholic molecules as indicated by experiments III and IV, which is indicated by the negative concentration changes of alcohol in the supernatant after the addition of host. It should be noted that the positive concentration changes found for ethanol are consistent with the partial dissociation of ethanol from the channels into the supernatant solution. A slightly higher final concentration of acetonitrile indicates the absence of any binding as this value is within the experimental error. Experiments I and II show a clear preference for small alcohols with high selectivity toward methanol. Little competition is observed among C3 and C4 alcohols and C5 and C7 alcohols as indicated by experiments I and V, respectively. It can be deduced that the overall order of alcohol selectivity by this material is: C1, C2 > C3, C4 > C5, C7, which is in qualitative agreement with that expected on the basis of a shape- and size-selective inclusion process. The absence of any competition from molecules without the hydroxyl functionality confirms the NMR results, and points to a guest binding mechanism involving not only shape and size selectivity of incoming guests but also selectivity that is based on their electronic character and its complimentarity to the electronic and intermolecular bonding requirements of the channels.

Structural Rigidity and Integrity of the Zn−BTC Framework. The multidentate functionality of BTC and its ability to hold together a total of three pairs of zinc(II) centers lead to a rigid framework having unique stability toward inclusion. The aggregation of metal ion centers around BTC also prevents interpenetration of the Zn−BTC porous network due to the bulk associated with such structural organization. The use of inorganic clusters and hydrogen-bonded guest aggregates has been shown to be effective in reducing or preventing interpenetration in frameworks with large voids.[11]

Immersing large cube-shaped crystals of the unevacuated solid in DMF gave a solid that was formulated by elemental analysis as $Zn_2(BTC)(NO_3)\cdot(H_2O)_{0.5}(C_2H_5OH)_{0.5}(DMF)_{2.5}$. The presence of DMF and smaller amounts of ethanol was confirmed by solid-state NMR, which showed strong resonances due to DMF and relatively weaker resonances due to ethanol. The crystals were found to preserve their crystallinity and morphology even after the inclusion of DMF, which provided an opportunity to evaluate the framework rigidity of this material. Comparison of the XRPD pattern of the DMF-treated solid to that of the unevacuated material confirmed that the structural integrity of its framework is maintained, as indicated by the minimal differences in intensity and line width (Figure 3). Further examination of the pattern reveals a small but significant negative shift in the *d*-spacings, which has been used to calculate the new crystallographic cell length. This was found to be 14.266 Å

(11) (a) Yaghi, O. M.; Sun, Z.; Richardson, D. A.; Groy, T. L. *J. Am. Chem. Soc.* **1994**, *116*, 807−808. (b) Yaghi, O. M.; Li, H *J. Am. Chem. Soc.* **1995**, *117*, 10401−10402.

compared to 14.728(2) Å for the unevacuated solid, thus indicating a compression of the cubic cell by 0.462 Å upon DMF binding. The magnitude of this structural response to binding is similar to that observed in the well-studied zeolite RHO. The flexibility of its aluminosilicate framework ranges from 0.1 to 1.0 Å depending on the cation size and reaction temperature.[12]

At the outset of this study, reports on open framework 3-D porous coordination solids have been limited to materials that either have fragile frameworks, which collapse into nonporous condensed phases upon removal or exchange of their guest inclusions, or possess smaller pore size due to extensive interpenetration of their porous networks. The reversible binding of guests into the Zn−BTC framework and the preservation of its structural integrity are supported by a number of observations (see the Experimental Section). First, in spite of the lower intensity and broadened nature of the XRPD of the evacuated solid, $Zn_2(BTC)(NO_3)\cdot(H_2O)_{0.5}(C_2H_5OH)$, the most intense lines remain identifiable and their positions are comparable to those observed for the original, unevacuated, crystalline solid. By exposing the evacuated solid to ethanol, considerable sharpening of the XRPD lines is observed, indicating the absence of any major deformation of its Zn−BTC framework. The preparation and characterization of $Zn_2(BTC)(NO_3)\cdot(H_2O)_{0.5}(C_2H_5OH)_{0.5}(DMF)_{2.5}$ including its XRPD pattern, just presented, lend further support to the stability of the framework. Second, the demonstrated success of dynamic exchange cycles involving the absorption−desorption and reabsorption-desorption of methanol, ethanol, 1-propanol, and DMF indicate a reversible process occurring without destruction of the framework. Third, the facile nature of the inclusion process, in that it is completed immediately upon immersion of the solid, excludes the possibility of the solid dissolving and recrystallizing with the incoming guest species. The absence of molecular BTC or M−BTC species from the supernatant of the heterogenous host/guest mixture indicates that the framework building units do not dissociate during the inclusion process.

It is interesting to note that the Zn−BTC network described in this paper can be derived from the chiral Si net in $SrSi_2$,[13] where the Si atoms have alternately been replaced by the three-connected trigonal bipyramid, discussed above, and the trifunctional BTC building blocks. The large size of the building units results in an open framework with chiral channels. We are currently focusing on producing bulk samples of enantiomeric purity for their possible utility in separations.

(12) (a) Corbin, D. R.; Abrams, L.; Jones, G. A.; Eddy, M. M.; Harrison, W. T. A.; Stucky, G. D.; Cox, D. E. *J. Am. Chem. Soc.* **1990**, *112*, 4821−4830. (b) Parise, J. B.; Corbin, D. R.; Gier, T. E.; Harlow, R. L.; Abrams, L.; Von Dreele, R. B. *Zeolites* **1992**, *12*, 360−368.

(13) O'Keeffe, M.; Hyde, B. G. *Crystal Structures: I. Patterns and Symmetry*; Mineralogical Society of America: Washington, DC, 1996.

Summary

The use of triethylamine as noncoordinating base for the deprotonation of 1,3,5-benzenetricarboxylic acid in its room-temperature reaction with zinc(II) ethanolic solutions is critically important in achieving the 3-D porous framework, $Zn_2(BTC)(NO_3)\cdot(H_2O)(C_2H_5OH)_5$. The Zn−BTC framework supports a 3-D channel system of 14 Å cross-section that is occupied by highly mobile ethanol and water guest molecules as evidenced by thermogravimetric and solid-state NMR measurements. The multidentate functionality of BTC imparts rigidity and stability to the resulting porous framework, even in the absence of guests, thus allowing examination of its inclusion chemistry. Results from solid-state NMR (^{13}C CP MAS and static ^{13}C) and GC experiments reveal that the framework is highly selective toward the binding of alcohols—a process that occurs reversibly and without compromising the structural integrity of the 3-D porous network.

The demonstrated utility of multidentate building blocks in the construction of rigid, stable, and noninterpenetrated 3-D porous coordination networks has significant implications on the development of the zeolitic properties of these materials, as exemplified by the selective binding behavior exhibited by the Zn−BTC framework. This study advances the principles of using the molecular building block approach for the construction of functional porous extended solids. Furthermore, it illustrates the relevance of coordination chemistry in providing opportunities for accessing metal centers within such networks, which has led to an inclusion process that is based not only on the size and shape of the incoming guests but also on their affinity toward the metal center environment.

Acknowledgment. The financial support of this work by the National Science Foundation (Grant CHE-9522303) and the technical assistance of Dr. Ronald Nieman in collecting the NMR data, Dr. James Lehman in setting up the GC experiments, and Dr. Thomas L. Groy in writing the computer code to calculate the pore volume are gratefully acknowledged.

Supporting Information Available: Crystallographic data for $Zn_2(BTC)(NO_3)\cdot(H_2O)\ (C_2H_5OH)_5$ including a crystal structure analysis report and tables of positional parameters, thermal parameters, and interatomic distances and angles (24 pages). See any current masthead page for ordering and Internet access instructions.

JA9639473